SRC TR 87-123R1

Neural Networks for Tactile Perception

By

Y.C. Pati, D. Friedman,
P.S. Krishnaprasad, C.T. Yao,
M.C. Peckerar, R. Yang,
and C.R.K. Marrian

Report Documentation Page

Form Approved
OMB No. 0704-0188

1. REPORT DATE	2. REPORT TYPE	3. DATES COVERED
1987		**00-00-1987 to 00-00-1987**

4. TITLE AND SUBTITLE	5a. CONTRACT NUMBER
Neural Networks for Tactile Perception	5b. GRANT NUMBER
	5c. PROGRAM ELEMENT NUMBER
6. AUTHOR(S)	5d. PROJECT NUMBER
	5e. TASK NUMBER
	5f. WORK UNIT NUMBER
7. PERFORMING ORGANIZATION NAME(S) AND ADDRESS(ES) **University of Maryland,Electrical Engineering Department,College Park,MD,20742**	8. PERFORMING ORGANIZATION REPORT NUMBER
9. SPONSORING/MONITORING AGENCY NAME(S) AND ADDRESS(ES)	10. SPONSOR/MONITOR'S ACRONYM(S)
	11. SPONSOR/MONITOR'S REPORT NUMBER(S)

12. DISTRIBUTION/AVAILABILITY STATEMENT
Approved for public release; distribution unlimited

13. SUPPLEMENTARY NOTES

14. ABSTRACT
see report

15. SUBJECT TERMS

16. SECURITY CLASSIFICATION OF:			17. LIMITATION OF ABSTRACT	18. NUMBER OF PAGES	19a. NAME OF RESPONSIBLE PERSON
a. REPORT **unclassified**	b. ABSTRACT **unclassified**	c. THIS PAGE **unclassified**		**19**	

Neural Networks for Tactile Perception

Y. C. Pati* D. Friedman† P. S. Krishnaprasad* C. T. Yao‡
M.C. Peckerar R. Yang* C. R. K. Marrian

Systems Research Center and Dept. of Electrical Engineering
University of Maryland
College Park, MD., 20742
and
U.S. Naval Research Laboratory
Code 6804
Washington D.C., 20375

1. Introduction

Integrated tactile sensors appear to be essential for dextrous control of multifingered robotic hands. Such sensors would feature (1) compliant contact surfaces, (2) high resolution surface stress transduction, (3) local signal conditioning, and (4) local computation to recover contact surface stress. The last-mentioned item pertains to the basic inverse problem of tactile perception and the real time solution of this inverse problem is our primary concern. We think that good solutions to this problem (i.e. algorithms + implementations) will be needed for realizing dextrous hand control via tactile servoing. In this paper we describe a processor chip designed to solve the mathematical inversion problem utilizing neural network principles. An energy function for the network is derived and we show that the equilibrium states are just regularized solutions to the inversion problem. Simulations indicate that this chip can function in the presence of large amounts of electrical noise. In addition the effect of processing induced variability in sensor response can also be minimized using the maximum entropy estimate method described below.

The tactile sensor design we refer to is the one reported in [1]. This particular design is based on piezo-resistive transduction via an array of diffuse resistors in silicon. Surface load on a compliant layer is transformed into resistance changes proportional to triaxial strains. Initial testing of the sensor has yielded repeatable, linear characteristics. The signal conditioning chip which acts as an interface between the sensor array and subsequent processor chips has also been fabricated.

The outline of this paper is as follows. In the next section we describe a model for the compliant contact layer. The algorithm for deconvolution and the network implementation proposed are described in section 3. A detailed analysis of the stability and convergence properties of the network is presented in section 4. The neural network chip described in this paper has been simulated at the system level. The simulation results for this network based on a particular linear elastic model (described in section 2) of the compliant contact layer. We consider in the simulations some of the errors introduced by process variability in VLSI implementation. We include a comparision to Fourier deconvolution in the presence of noise. The simulations carried out using SIMNON a general purpose nonlinear simulation package developed at Lund Institute of Technology, Sweden (kindly provided us by Professor Astrom), are described in section 5.

*supported in part by NSF under grant OIR-85-00108
†also Harvard University,Cambridge,MA.
‡Sachs Freeman Associates, Landover MD.

2. The Elastic Model

We model the compliant contact layer as a homogeneous, isotropic, linear elastic half-space. The standard stimulus used is a cylindrical indenter viewed as a line load. The relationship between surface stress and strains at a fixed depth (see fig 1) is given by a convolution operator. A model of this type is considered by Hollerbach and Fearing in their paper [2] and a careful study of related inverse problems is to be found in the thesis of Yang [3]. Assuming a plane strain condition in the layer and Poisson's ratio of 0.5 (as for rubber-like materials), the integral operator relating the surface stress to strain at a depth x is given by

$$\epsilon_x(y) = \int_{-\infty}^{\infty} t(x, y - y_0) f_v(y_0) dy_0. \tag{2.1}$$

Where,

$$t(x, y - y_0) = \frac{3}{2\pi E} \frac{x(x^2 - (y - y_0)^2}{(x^2 + (y - y_0)^2)^2} \tag{2.2}$$

and E is the elastic modulus of the compliant material.

The tactile sensor measures a spatial sampling of the strain $\epsilon_x(y)$ at intervals of $\Delta (= y_{i+1} - y_i)$. The basic inverse problem (planar version) of tactile perception is to recover the surface stress $f_v(y)$ or a sampled version of it from the strain data. The problem is ill-posed in the sense of Hadamard since the convolution operator has only a densely defined inverse operator. The discrete (or sampled) inverse problem is one of solving a linear equation associated to the discrete convolution. We write this as

$$\mathbf{T}\,\vec{f} = \vec{\epsilon}, \tag{2.3}$$

where the matrix **T** of weights is determined by the convolution kernel in an obvious manner. Inverse problems of this type have been studied extensively in many areas of applied mathematics using regularization techniques. The specifics of the tactile sensing context have been treated in Yang [3]. In the present paper we give a solution to the discrete inversion problem using a highly interconnected network of simple analog processors (i.e. a neural network).

3. A Neural Network

Inspired by the previous work of Tank and Hopfield [4], on neural networks for solving certain optimization problems, we propose a design as in Figure 2 for solving the deconvolution problem of tactile perception. A complete description of this network is presented in Marrian and Peckerar [5]. The input currents (I_i) are the measured strains. The essential difference between our design and that of Tank-Hopfield is in the use of exponential amplifiers in the signal plane and the introduction of the convolution kernel as the interconnection matrix. We show in section 4 that under suitable hypotheses, the network relaxes to a solution of eqn 2.3.

As in the Tank Hopfield net [5], the network can be considered as consisting of a signal plane and a constraint plane. The output of the signal plane represents the current 'guess' at the surface stress. The constraint plane 'evaluates' the output of the signal plane to determine the degree to which the guess violates eqn. 2.3. The outputs of the constraint plane readjust the signal plane outputs so long as equation 2.3 is violated. The use of exponential amplifiers in signal plane results in the introduction of a term proportional to the negative of the information theoretic (or Shannon) entropy into the energy function for the network. Thus equilibrium states of the network correspond to entropy maxima as well. In situations where noise levels are sufficient to severely corrupt the validity of a solution, the network settles to the solution which maximizes Shannon entropy. Hence we shall refer to this network as a *maximum entropy deconvolution network.*

4. Convergence and Equilibria

The maximum entropy deconvolution network is a special case of the general non-linear RLC networks considered by Brayton and Moser [8], Millar [9], and Cherry [10]. In this section we examine the conditions subject to which all solutions to the governing differential equations for the network approach equilibrium solutions as $t \to \infty$. We also define a function $P(u^*)$ and show it to be a strict Liapunov function for the network.

We first restate and prove two theorems. The first of these theorems is known as Tellegen's theorem [11], but is presented as in [8] so as to have a geometrical interpretation. The second theorem is stated by Brayton and Moser in [8].

For the network shown in figure 2, a complete set of variables (see [8]) can be defined as $u^* = (u_1, u_2, \ldots, u_N)$ where u_i is the voltage across the capacitor in the ith signal plane node. The set of variables $u_1, \ldots, u_N$ is complete in the sense that the u_i can be chosen independently without violation of Kirchoff's laws and that they determine in each branch of the network at least one of the two variables, branch current or branch voltage.

We consider a network composed of branches and nodes with the restriction that a branch connects exactly two nodes. Arbritrarily assigning a direction to the branch currents, we define i_μ as the current flowing from the initial node to the end node of the μth branch in the network. The branch voltage v_μ is defined as the voltage rise measured from the end node to the initial node of the μth branch in the network.

In such a directed network with b branches and m nodes, the set of branch currents $i = (i_1, ..., i_b)$ and the set of branch voltages $v = (v_1, ..., v_b)$ are vectors in a b-dimensional Euclidean vector space $\mathcal{E}^b$ with the inner product defined by $(x, y) = \sum_{\mu=1}^{b} x_\mu y_\mu$. Let $\mathcal{I}$ be the set of all vectors in $\mathcal{E}^b$ such that if $i \in \mathcal{I}$ then the constraint of Kirchoff's current law is satisfied for each node in the network, i.e. $\sum_{node} i_\mu = 0$. Similarly, let $\mathcal{V}$ be the set of all vectors in $\mathcal{E}^b$ such that if $v \in \mathcal{V}$ then Kirchoff's voltage law is satisfied, i.e $\sum_{loop} v_\mu = 0$. $\mathcal{I}$ and $\mathcal{V}$ are clearly subspaces of $\mathcal{E}^b$ since they are defined via linear relationships (Kirchoff's Laws). The following theorem shows that $\mathcal{I}$ and $\mathcal{V}$ are orthogonal subspaces of $\mathcal{E}^b$.

Theorem 1(Tellegen's Theorem)

If $i \in \mathcal{I}$ and $v \in \mathcal{V}$ then

$$(i, v) = 0. \tag{4.4}$$

Proof:

Let $(V_1, ..., V_n)$ be the set of node voltages such that v is the vector of voltage differences between the end nodes and the initial nodes of each branch. let i_{kl} be the current from node k to node l. Then if the branch connecting node k to node l is labeled as the μth branch,

$$v_\mu i_\mu = (V_k - V_l) i_{kl} = (V_l - V_k) i_{lk} \tag{4.5}$$

Due to the symmetry in k and l,

$$\begin{aligned} \sum_{\mu=1}^{b} v_\mu i_\mu &= \frac{1}{2} \sum_k \sum_l (V_k - V_l) i_{kl} \\ &= \frac{1}{2} \left(\sum_k V_k \sum_l i_{kl} - \sum_l V_l \sum_k i_{kl} \right) \end{aligned}$$

but,

$$\sum_l i_{kl} = \sum_{node\ k} \pm i_\mu \tag{4.6}$$

and

$$\sum_k i_{kl} = \sum_{node\ l} \pm i_\mu. \tag{4.7}$$

Since the branch currents in the network must satisfy Kirchoff's current law we know $\sum_{node} \pm i_\mu = 0$. Therefore

$$\sum_{\mu=1}^{b} v_\mu i_\mu = 0 \tag{4.8}$$

Theorem 2

Let Γ denote a one dimensional curve in $I \times \mathcal{V}$ with coordinates denoted by i and v. Then,

$$\int_\Gamma \sum_{\mu=1}^{b} v_\mu di_\mu = \int_\Gamma \sum_{\mu=1}^{b} i_\mu dv_\mu = 0 \tag{4.9}$$

Proof: Since $(di_1, \ldots, di_b) \in I$,

$$(v, di) = \sum_{\mu=1}^{b} v_\mu di_\mu = 0 \qquad \text{(By Tellegen's theorem).} \tag{4.10}$$

Integrating the above sum along Γ we get,

$$\int_\Gamma \sum_{\mu=1}^{b} v_\mu di_\mu = 0. \tag{4.11}$$

Integrating by parts we see that,

$$(v, i)\Big|_\Gamma - \int_\Gamma \sum_{\mu=1}^{b} i_\mu dv_\mu = 0. \tag{4.12}$$

By Tellegen's theorem we know $(v, i) = 0$, therefore,

$$\int_\Gamma \sum_{\mu=1}^{b} i_\mu dv_\mu = 0 \tag{4.13}$$

Having stated the above two theorems and having defined the complete set of variables $u* = (u_1, \ldots, u_N)$ for the network, we proceed with the definition of a mixed potential function.

From theorem 2 we know that $\int_\Gamma \sum_{\mu=1}^{b} v_\mu di_\mu = 0$. We choose Γ from a fixed initial point to a variable end point in $\mathcal{E}^b$ such that along Γ the characteristic relationships of the constituent elements of the network are satisfied. We can write equation (4.11) in the following form:

$$\int_\Gamma \sum_{\rho=1}^{N} v_\rho di_\rho + \int_\Gamma \sum_{\mu=N+1}^{b} v_\mu di_\mu = 0 \tag{4.14}$$

The first integral is over all capacitive branches and the second is over all other branches. Integrating the first integral by parts we get,

$$P + \int_\Gamma \sum_{\rho=1}^{N} i_\rho dv_\rho = 0, \tag{4.15}$$

where ,

$$P = -\left[\int_\Gamma \sum_{\mu=N+1}^{b} v_\mu di_\mu + \sum_{\rho=1}^{N} i_\rho v_\rho \Big|_\Gamma\right]. \tag{4.16}$$

Therefore from (4.15) we also have,

$$P = -\int_\Gamma \sum_{\rho=1}^{N} i_\rho dv_\rho. \tag{4.17}$$

Let

$$\xi = \sum_{\rho=1}^{N} i_\rho dv_\rho. \tag{4.18}$$

We now establish the conditions for ξ to be integrable i.e the conditions for the line integral (4.17) defining P to be independent of the path of integration Γ.

For (4.17) to be independent of Γ, it is necessary that ξ be a perfect differential. That is, we can write ξ as,

$$\xi = d\sigma, \tag{4.19}$$

where $\sigma = \sigma(v_1, \ldots, v_N)$ and,

$$d\sigma = \frac{\partial \sigma}{\partial v_1} dv_1 + \cdots + \frac{\partial \sigma}{\partial v_N} dv_N. \tag{4.20}$$

But since $\xi = d\sigma$ we have,

$$d\sigma = i_1 dv_1 + \cdots + i_N dv_N. \tag{4.21}$$

Comparing (4.20) and (4.21) we get,

$$i_\rho = \frac{\partial \sigma}{\partial v_\rho} \qquad \rho = 1, \ldots, N. \tag{4.22}$$

Therefore

$$\frac{\partial i_\rho}{\partial v_\eta} = \frac{\partial^2 \sigma}{\partial v_\rho \partial v_\eta} = \frac{\partial i_\eta}{\partial v_\rho} \quad \eta, \rho = 1, \ldots, N. \tag{4.23}$$

From the above equation (4.23) we see that in order for (4.17) to be independent of Γ, the following must hold:

$$\frac{\partial i_k}{\partial v_j} = \frac{\partial i_j}{\partial v_k} \qquad j, k = 1, \ldots, N. \tag{4.24}$$

If (4.24) holds then P is a function of the endpoints of Γ alone.

Assuming that the line integral (4.17) is independent of path we can write the following equations for the current in the capacitive branches:

$$i_\rho = -\frac{\partial P}{\partial v_\rho} \qquad \rho = 1, \ldots, N. \tag{4.25}$$

However, we know from the the dynamical law of capacitors that,

$$i_\rho = C_\rho \frac{dv_\rho}{dt} \qquad \rho = 1, \ldots, N. \tag{4.26}$$

Therefore,

$$C_\rho \frac{dv_\rho}{dt} = -\frac{\partial P(v)}{\partial v_\rho} \quad \rho = 1, \ldots, N \tag{4.27}$$

where $v = (v_1, \ldots, v_N)$. We now write the system of differential equations defining the dynamical behavior of the network in the following vector form,

$$-C\dot{x} = \frac{\partial P(x)}{\partial x} \tag{4.28}$$

where $x = v$, $C = diag(C_1, ..., C_N)$, and $\frac{\partial P(x)}{\partial x}$ is the gradient of $P(x)$. The following theorem relates $P(x)$ to the equilibrium states of the network.

Theorem 3

Let

$$\frac{dx}{dt} = -B\frac{\partial G(x)}{\partial x} \qquad x \in U \qquad G : U \to \Re \tag{4.29}$$

where U is a normed vector space and B is a positive definite, diagonal, $n \times n$ matrix. Then $\frac{d}{dt}G(x(t)) \leq 0$ for all $x \in U$ and $\frac{d}{dt}G(x(t)) = 0$ if and only if x is an equilibrium of the gradient system (4.29). Proof:

Taking the time derivative of G along trajectories,

$$\begin{aligned} \frac{dG(x)}{dt} &= (\frac{\partial G(x)}{\partial x}, \frac{dx}{dt}) \\ &= (\frac{\partial G(x)}{\partial x}, -B\frac{\partial G(x)}{\partial x}) \\ &= -B\left|\frac{\partial G(x)}{\partial x}\right|^2 \end{aligned}$$

Since B is positive definite, this completes the proof.

Corollary: If $\tilde{x}$ is an isolated minimum of $G(x)$ then $\tilde{x}$ is an asymptotically stable equilibrium of the gradient system (4.29).

As the matrix C is positive definite, it is obvious that the function $P(x)$ which we shall call the mixed potential function, decreases along solutions to (4.28) except at equilibrium points. Therefore the equilibrium states of the network correspond to stationary points of $P(x)$ and the local minima of $P(x)$ are the stable equilibria. If in addition to this $P(x) \to \infty$ as $|x| \to \infty$ then it can be shown that all solutions to (4.28) approach one of the set of equilibrium solutions as $t \to \infty$.

$P(x)$ is just the negative of the 'co-content' (as defined by Milar) of all the capacitive elements in the network. In [9] Milar shows that the total co-content, which is the sum of the cocontents of all constituent elements of the network, is an invariant of motion. That is, the total co-content is a conserved quantity. The analogy to energy of a particle in motion is evident. For a moving particle the total energy, taken as the sum of the kinetic and potential energy, is an invariant of motion and equilibria represent local minima of potential energy. Therefore $P(x)$ can be regarded as a type of potential energy function for the network.

(Energy Function for Deconvolution Network)

We now discuss the application of the potential function defined in (4.17) to the maximum entropy deconvolution network. In the following we assume that for the network in figure 2, any dynamics associated with the constraint plane can be neglected. This assumption is valid if the response of the amplifiers in the signal plane is sufficiently slower than of those of the constraint plane. It is intuitively obvious that a 'potential' function should depend only upon the current state of the network and the fixed 'zero' reference potential chosen (i.e. it should depend only upon the endpoints of Γ). To establish the path independence of the integral in (4.17) we turn to the 'mixed-partials' condition of (4.24).

The current through the capacitor connected to the nth signal plane node is given by,

$$i_n = C\frac{du_n}{dt} = -\frac{u_n}{R} - \frac{1}{R} - \sum_k t_{kn} f(T_k \cdot v - I_k) - \alpha(\sum_k v_k - 1). \tag{4.30}$$

Here $T_k = (t_{k1}, t_{k2}, \ldots, t_{kN})^T$ and α is the gain of the normalization amplifier in the constraint plane. Since $u_n = g^{-1}(v_n)$ we can write,

$$i_n = C\frac{du_n}{dt} = -\frac{g^{-1}(v_n)}{R} - \frac{1}{R} - \sum_k t_{kn} f(T_k \cdot v - I_k) - \alpha(\sum_k v_k - 1). \tag{4.31}$$

The potential function P is thus a function of $v = (v_1, \ldots, v_N)^T$ i.e. we can use v as an alternate set of independent variables and

$$P(v) = -\int_\Gamma \sum_n i_n dv_n. \tag{4.32}$$

From (4.31) we see that,

$$\frac{\partial i_n}{\partial v_j} = \frac{\partial}{\partial v_j}\left(-\sum_k t_{kn} f(T_k \cdot v - I_k) - \alpha(\sum_k v_k - 1)\right) \tag{4.33}$$

$$= -\sum_k t_{kn} t_{kj} - \alpha \qquad k, j, n = 1, \ldots, N \tag{4.34}$$

and,

$$\frac{\partial i_j}{\partial v_n} = \frac{\partial}{\partial v_n}\left(-\sum_k t_{kj} f(T_k \cdot v - I_k) - \alpha(\sum_k v_k - 1)\right) \tag{4.35}$$

$$= -\sum_k t_{kj} t_{kn} - \alpha \tag{4.36}$$

$$= \frac{\partial i_n}{\partial v_j} \qquad k, j, n = 1, \ldots, N. \tag{4.37}$$

Thus the conditions of (4.24) are satisfied.

We can now write the dynamical equations of the network in the following form:

$$\frac{du}{dt} = -C^{-1}\frac{\partial P(v(u))}{\partial v(u)} \tag{4.38}$$

where $v = (v_1 \ldots, v_N)$ and $v_n = g^{-1}(u_n)$. Since $v_i = g(u_i)$, we have:

$$\frac{dv}{dt} = -GC^{-1}\frac{\partial P(v)}{\partial v}, \tag{4.39}$$

where $G = diag(g'(u_1), \ldots, g'(u_N))$. Because $g(u) = \exp(u)$, we know that G is always positive definite.

Applying theorem 3 to (4.39), it is clear that the network will relax to one of the local minima of $P(v)$. In order to understand the nature of the stable equilibrium states of the network we must evaluate the integral expression for P.

$$P(v) = \int_\Gamma \sum_n \left(\frac{g^{-1}(v_n)}{R} + \frac{1}{R} + \sum_k t_{kn} f(T_k \cdot v - I_k) + \alpha(\sum_k v_k - 1)\right) dv_n \tag{4.40}$$

Choosing 0 as the starting point of the path Γ, we can write (4.40) as,

$$\sum_n \int_0^{v_n} \frac{g^{-1}(v_n)}{R} dv_n + \sum_n \int_0^{v_n} \frac{dv_n}{R} + \int_\Gamma \sum_n \sum_k t_{kn} f(T_k \cdot v - I_k) dv_n + \sum_n \int_\Gamma \alpha(\sum_k v_k - 1) dv_n. \quad (4.41)$$

If we let $F(z_k)$ be such that $dF(z_k)/dz_k = f(z_k)$, $(z_k = (T_k \cdot v - I_k))$ then,

$$P(v) = \sum_n \int_0^{v_n} \frac{g^{-1}(v_n)}{R} dv_n + \sum_n \frac{v_n}{R} + \sum_k F(T_k \cdot v - I_k) + \alpha(\sum_k v_k - 1)^2. \quad (4.42)$$

For the deconvolution network shown in figure 2 the signal plane amplifiers are characterized by $g(u) = \exp(u)$. Therefore

$$\int_0^{v_n} \frac{g^{-1}(v_n)}{R} dv_n = v_n \log v_n - v_n \quad (4.43)$$

From figure 2 we also see that the constraint plane amplifiers characteristics are given by:

$$f(z) = sz \quad (4.44)$$

where s is a constant defining the feedback gain. We can thus define the function $F(T_k \cdot v - I_k)$ by,

$$F(T_k \cdot v - I_k) = s(T_k \cdot v - I_k)^2 \quad (4.45)$$

From (4.42) and (4.43),

$$P(v) = \frac{1}{R} \sum_n v_n \log v_n + \sum_k s(T_k \cdot v - I_k)^2 + \alpha(\sum_k v_k - 1)^2. \quad (4.46)$$

Equation (4.46) gives us an explicit form for the energy function for the maximum entropy deconvolution network which has been derived using nothing more than Kirchoff's laws. We observe from (4.46) that the network of figure 2 will settle to a state which minimizes the sum of the error in the estimate, the negative of the Shannon entropy and the deviation from a normalized solution. By varying the resistor R we can vary the weight given to the regularizing (entropy) term relative to the minimization of the square of the error. The constant α is used to adjust the weight given to the normalization which is necessary since there is no reason to believe that the solution should be normalized.

5. Simulation Results

The complexity of interconnections and feedback loops within the maximum entropy deconvolution neural network suggests the use of computer simulations for performance evaluation and optimization of design parameters.We have carried out extensive simulations to evaluate the performance of the network in such terms as convergence time, proximity of the solution to the true solution, noise immunity, etc. In addition we have considered the problems associated with the realities of fabrication of such a neural net as a stand-alone processor. These issues are discussed below.

From equation 2.2 the discrete convolution kernel is given by

$$T_{ij} = \frac{3}{2\pi E} \frac{x(x^2 - (y_i - y_j)^2}{(x^2 + (y_i - y_j)^2)^2}. \quad (5.47)$$

Thus the strain measured by a sensor at y_n (depth x) is given by the discrete convolution :

$$i(y_n) = \sum_{j=-K}^{K} T_{nj} f_v(y_j) \quad (5.48)$$

Where $f_v(y_j)$ is the vertical stress applied at the surface (tangential stress components are not considered here) and 2K+1 is the number of sample measurements (number of sensors). It is assumed that the sensors are uniformly distributed beneath the surface at spatial intervals Δ. The surface stress is designed to represent stress due to indentation of the surface with a cylindrical object (Conway et.al. [7]) i.e.,

$$f_v(y) = \begin{cases} \frac{p}{\pi a^2}\sqrt{a^2 - y^2} & \text{if } y \in [-a, a] \\ 0 & \text{elsewhere} \end{cases} \tag{5.49}$$

Where p is the normal force per unit length and a is the half-width of contact (strip contact is assumed for the one-dimensional setting).

The deconvolution network itself is modeled under the assumption that the system dynamics are contained entirely within the signal plane (i.e the response of the constraint plane amplifiers is instantaneous). Additional assumptions that are made in these simulations is that it is possible to realize a true exponential amplifier and that the desired constraint plane amplifier characteristics are physically attainable.

Shown in fig.3(a) is the time evolution of three of the outputs (o_{31}, o_{29} and o_{16}) of the maximum entropy network and the corresponding ideal solutions (fv_{31}, fv_{29} and fv_{16}) to the deconvolution problem. Fig.3(b) shows the resulting reconstruction (discrete) of the designed surface stress (continuous). Both speed and accuracy of the network are evident in these simulations. Perhaps the most striking (and useful) aspect of the proposed network, is its performance in the presence of noise. Shown in fig.4(b) is the reconstruction of surface stress using 41 sample strain measurements with white noise ($\sigma = 0.1$) added. Fig.4(c) shows reconstruction of the same designed surface stress under identical conditions using a discrete Fourier transform method which, in the absence of noise, produces an almost perfect reconstruction (Yang[3]).

Issues related to processing realities are critical in any attempt to implement a neural network-based circuit. To reduce the effect of processing-induced variations we consider an approach to the resistive network design problem using amorphous silicon as the resistor material [6]. This approach yields high resistance values and can be scaled very accurately in a discrete manner. All resistive connectors have a given value and are formed by opening fixed-sized contact between two conductor layers. The total conductance linking a pair of nodes, then, is proportional to the number of contact openings between those nodes. A small range of conductances is desirable because fewer resistor contacts means less used area (i.e., greater chip density) and less signal coupling. Since the network behavior is determined by the ratio of the conductances, rather than their absolute values, the process variation that causes the variation of the individual resistance can be neglected, so long as they are large enough. This approach, however, introduces new sources of error, namely, quantization and truncation errors. The effect of quantizing the interconnection values on output accuracy is therefore a topic that must be studied.

Simulations were performed to study the effect of quantization of the **T** matrix. Initial results of these simulations (using a 9-level quantization of the T_{ij} conductances) indicate errors introduced into the solution are no greater than 5% relative to the unquantized case. Studies of the Hopfield associative memory with as much as 20% random error introduced into the T_{ij}'s indicate robustness with respect to such processing induced variations. Future investigations will involve the extension of such robustness to the deconvolution network.

6. Discussion

We have proposed a solution to the basic inverse problem of tactile perception. The novelty of the solution lies in the implementation. Shannon entropy has in the past been successfully used as a regularizing principle in optical image reconstruction problems. However, regularizing principles of this nature have in most cases manifested as algorithms requiring fairly powerful digital computers for real-time implementation. Work is currently underway

at the microelectronics processing facility of the Naval Research Laboratory in Washington to implement the algorithm we propose on a VLSI chip.

The energy function for the network was derived using only the fundamental arguments of Kirchoff's laws and thus can be used for any general RC network satisfying the two hypotheses. The hypotheses are: (1) the mixed partials condition of equation 4.24 is satisfied, and (2) the matrix multiplying the gradient of P on the left in equation 4.39 is positive definite.

Preliminary simulation results are very promising. The average convergence time for the network is about 5 ms which is adequate for most real time applications. Although the reconstructions obtained are not perfect, the flexibility of VLSI implementation, rapid convergence and noise immunity are properties that may ,in practice, far outweigh absolute accuracy of the solution.

7. Conclusions

We have developed a software model of a neural net processor which has demonstrated the following:

- An ability to deconvolve the applied stress profile from strain measurements,
- An ability to perform this deconvolution in the presence of relatively large amounts of noise.

The simulated convergence time of the net is less than 5ms. for all cases studied. The net will make estimates of the true solution based on maximum entropy when noise levels do not permit Fourier deconvolutions to take place. The noise can be either electronic noise or 'fixed pattern' noise introduced by process variability.

We have also mathematically demonstrated the stability and convergence properties of the network and shown that the equilibria do indeed correspond to solutions of the deconvolution problem.

References

- [1] C. T. Yao, M. C. Peckerar, J. Wasilik, C. Amazeen and S. Bishop, "A Novel Three Dimensional Microstructure Fabrication Technique For A Triaxial Sensor Array", preprint, Naval Research Laboratory, Code 6804, Washington D.C.
- [2] Hollerbach and Fearing, "Basic Solid Mechanics For Tactile Sensing", Internatl. Journal of Robotics Research, Vol.4 No.3,Fall 1985
- [3] Rui Yang, "Tactile perception for Multifingered Hands", Master of Science Thesis, University of Maryland at College Park, August 1987
- [4] D. W. Tank and J. J. Hopfield, ", Simple Neural Optimization Networks:", IEEE Trans. on Circuits and Systems CAS-33, No. 5, 1986
- [5] C.R.K. Marrian and M.C. Peckerar, "Electronic Neural Net Algorithm For Maximum Entropy Deconvolution",Naval Research Laboratory, Wash. D.C. Presented at the IEEE First Annual Inter. Conf. On Neural Networks, San Diego, CA, June 1987
- [6] R. E. Howard, D. B. Schwartz, J. S. Denker, R. W. Epworth, H. P. Graf, W,. E. Hubbard, L. D. Jackel, B. L. Straughn, and D. M. Tennant, "An Associative Memory Based on an Electronic Neural Network Architecture", IEEE Trans. on Electron Devices, Vol. ED-34, No. 7, pp. 1553 - 1556, July, 1987.
- [7] H.D. Conway, et. al., Normal and Shearing Contact Stress in Indented Strips and Slabs", Int. Journal. of Eng. Sci. 4:343-359, 1966.

- [8] R. K. Brayton and J. K. Moser, A Theory Of Nonlinear Networks I and II, Quarterly Of Applied Mathematics, Vol XXII, April 1964.
- [9] W. Millar, Some General Theorems for Nonlinear Systems Posessing Resistance, Phil. Mag. 42 (1951) p.1150.
- [10] C. Cherry, Some General Theorems for Nonlinear Systems Posessing Reactance, Phil. Mag. 42 (1951) p.1161.
- [11] B. D. H. Tellegen, A General Network Theorem With Applications, Phillips Research Reports 7 (1952)

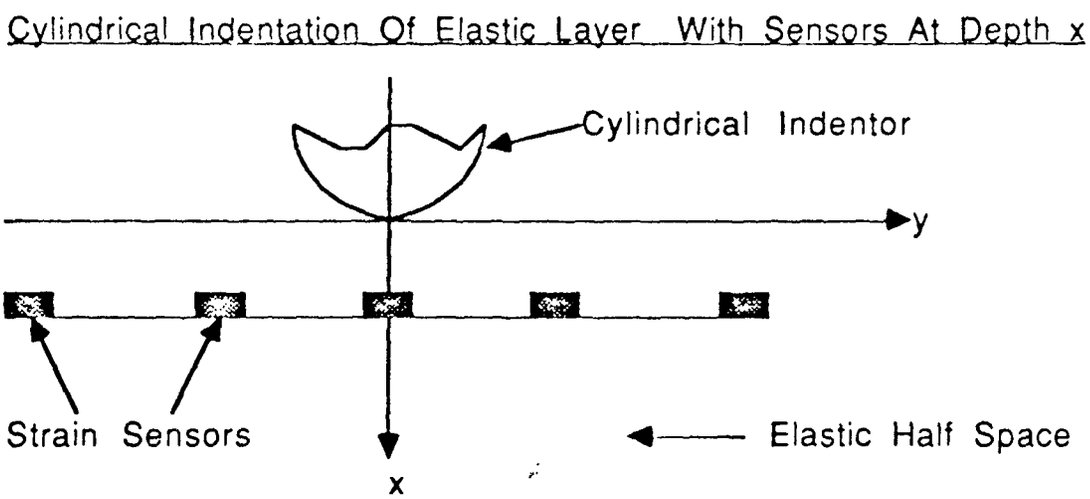

Figure 1

MAXIMUM ENTROPY DECONVOLUTION NETWORK WITH TWO CHANNELS

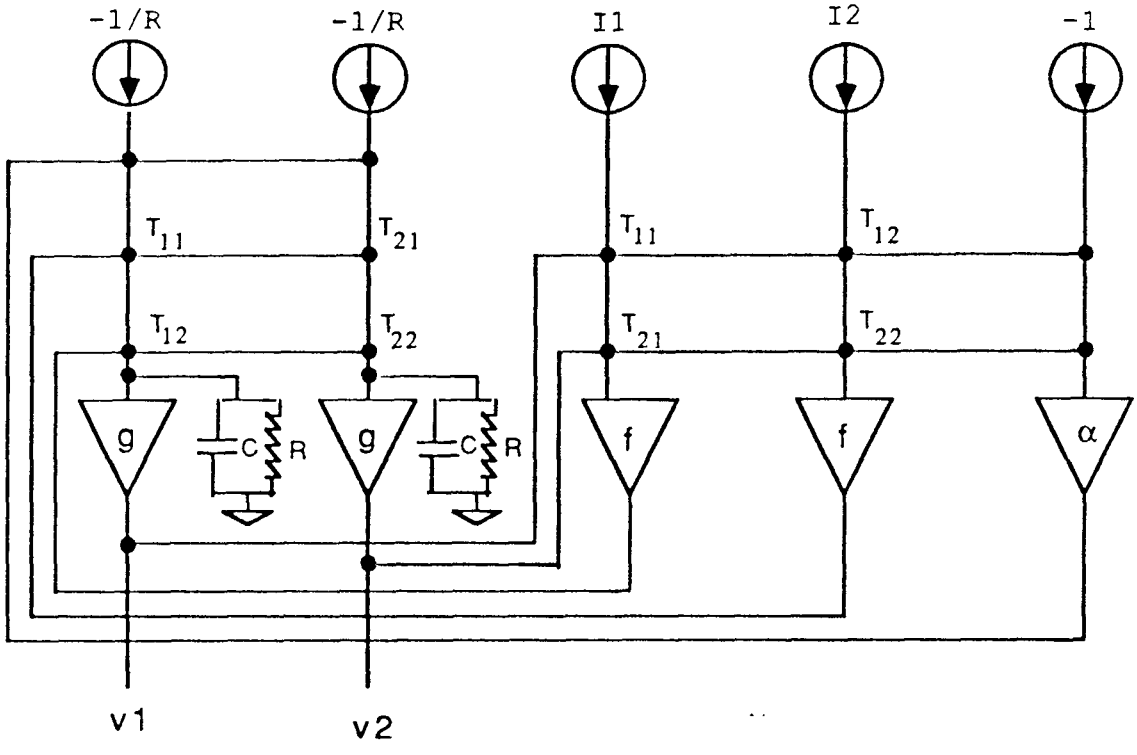

I_k are the measured strains.

V_k are the outputs of the network

T_{ij} are the elements of the convolution kernel.

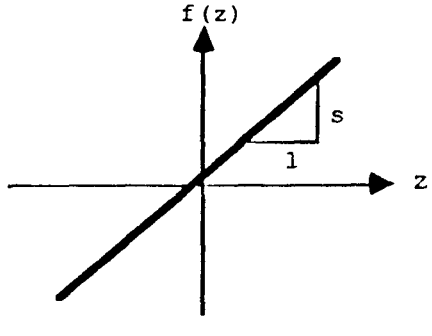

Constraint Node Characteristic

Figure 2

Fig. 3(a)time evolution of three outputs of deconvolution net (61 samples)

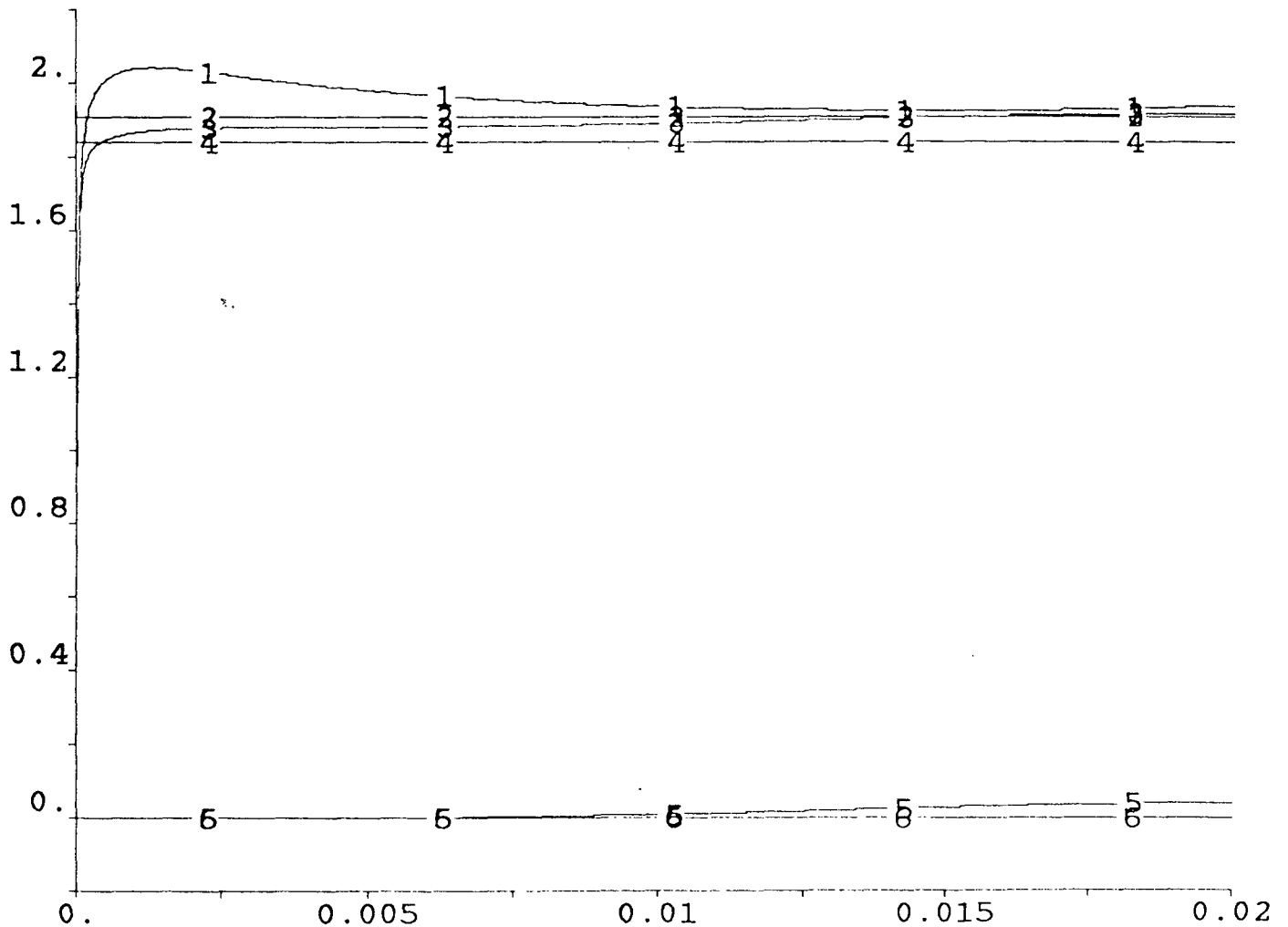

1) o31: 2) fv31 3) o29; 4) fv29; 5) o16; 6) fv16#

Fig. 3(b) reconstruction of surface stress (npts=61, w=8, eps=.1, no noise)

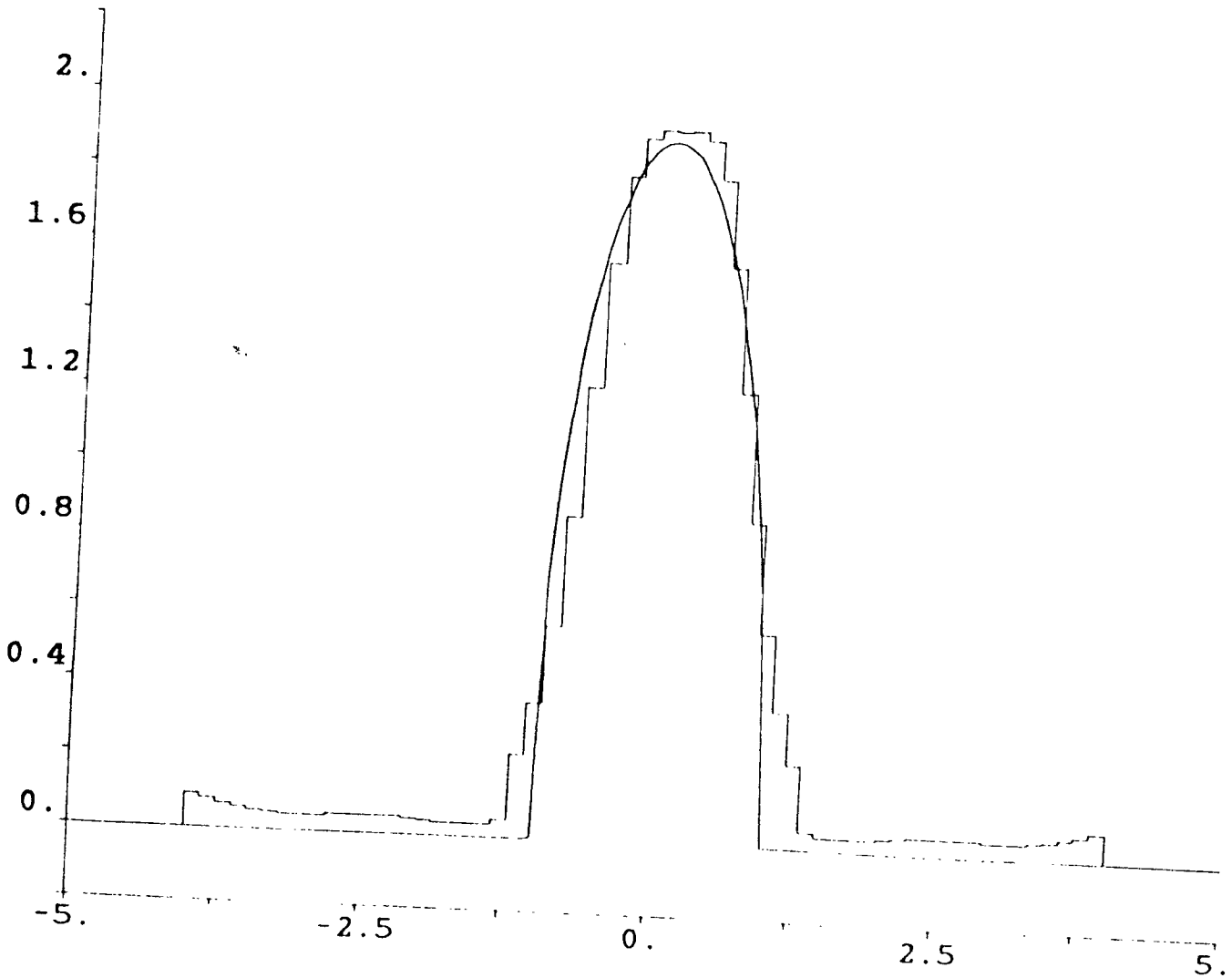

fig.4(a)time evolution of outputs of net with noise added (41 sample points used)

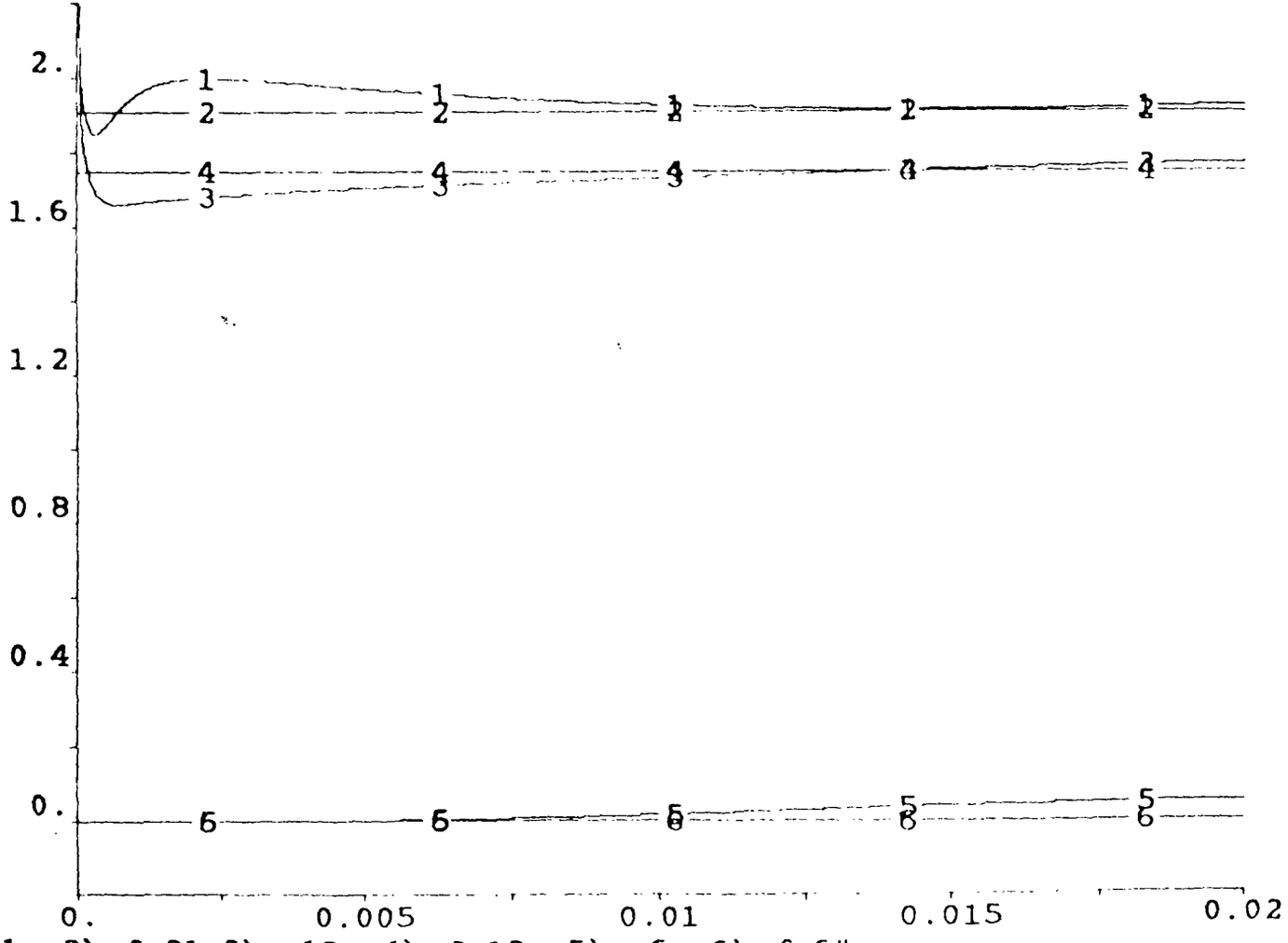

1) o21: 2) fv21 3) o19; 4) fv19; 5) o6; 6) fv6#

fig.4(b) reconstruction using 41 samples,noise (std dev =.1) added,w=8

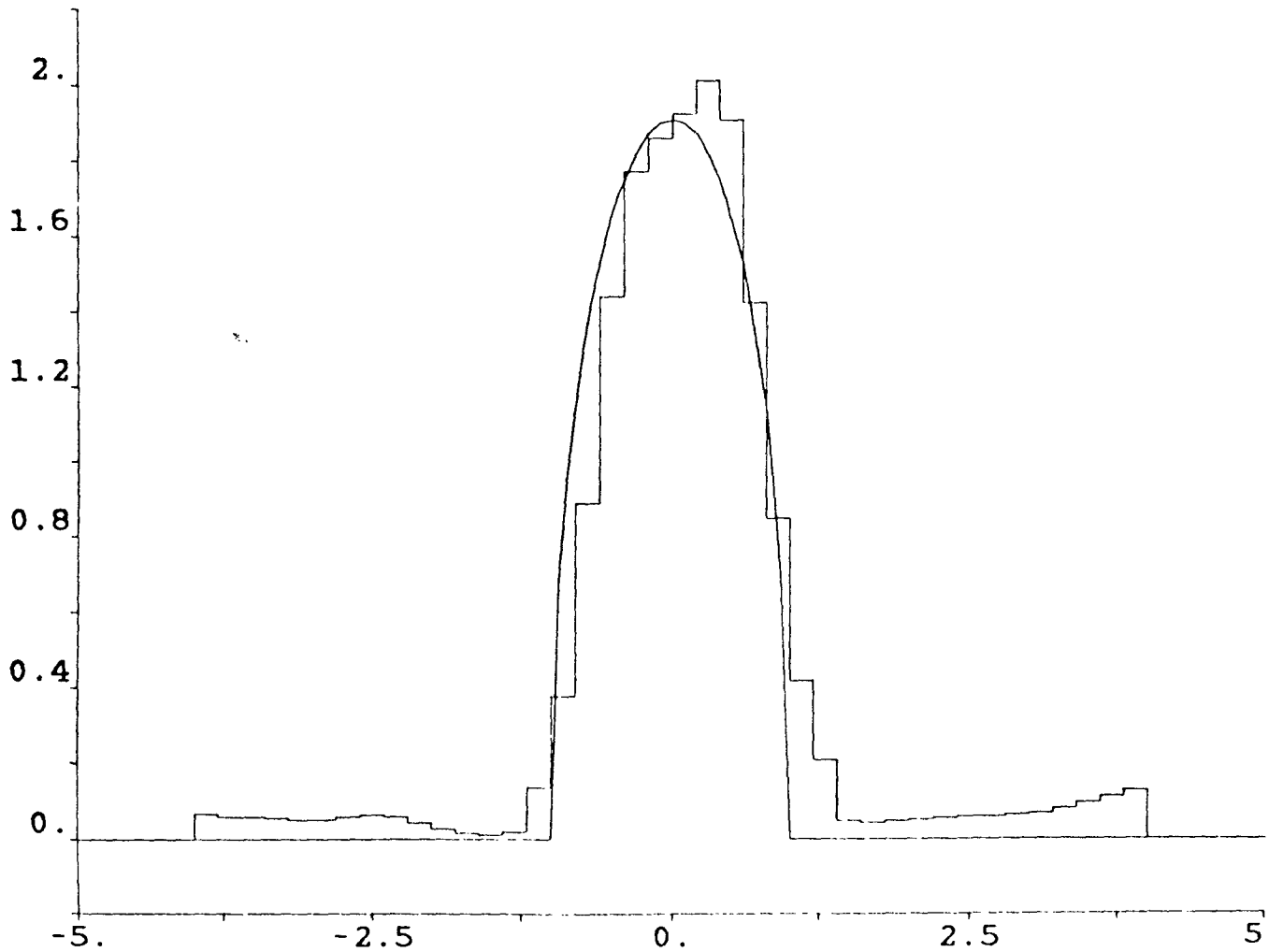

Maximum Entropy Deconvolution With Noise Added To Inputs

Figure 4(c) Fourier Deconvolution With Noise Added to Inputs